

Sinusoidal Dither in a Relay Feedback System

Lim L H, Loh A P*

email : elelohap@nus.edu.sg

Dept of Electrical & Computer Engineering
National University of Singapore

Abstract—This paper examines the effect of a sinusoidal dither in a relay feedback system. The use of dither in achieving signal stabilization and quenching of limit cycles is well known in nonlinear systems. The effect of dithering is a similar to that of forced oscillations where the external signal causes oscillations of the same frequency to occur in the system. This paper shows that FO of higher frequencies will produce a lower amplitude and achieve a reduction in the amplitude of oscillations for dither periods below a certain value, T_f^* . This idea is used to design a sinusoidal dither signal which results in reduced oscillation amplitudes. Analytical expressions for T_f^* are obtained for first and second order plants. For higher order systems, the Tsytkin Loci is used to identify T_f^* . Simulation studies are presented to illustrate the results.

Keywords: relay feedback systems, sinusoidal dither

I. INTRODUCTION

Switching is an important concept widely used to control certain behaviours in a device. In power electronics, for instance, switching is used effectively in the control of converters. The problem with switching, however, is that it causes great difficulties in the analysis of the behaviour in the overall nonlinear system, especially for discontinuous systems. For example, in the dithered RFS considered in Luigi Iannelli et al. [1], [2], only an approximate analysis was proposed despite having a very specific dither signal. Their analysis resulted in a lower bound of the dither frequency which guarantees the stability of the nonsmooth system. The final bound was also shown to be conservative.

To the best of our knowledge, and as pointed out in Pervozvanski and Canuda de Wit [3], a rigorous analysis for dithered discontinuous system such as that of a dithered RFS does not exist. The common approach is to approximate the original discontinuous dithered system with a smooth system. Stability can be proven for a sufficiently high dither frequency by the use of the classical averaging theory, formerly developed by Zames and Shneydor[4], [5], [6] for continuous nonlinear systems. Other related works can be found in Mossaheb[7], Luigi Iannelli et al.[8] and Lehman and Bass[9]. Their results showed that a sufficiently high frequency dither can reduce the limit cycles in the dithered system to a negligible ripple but exact conditions on the dither periods and amplitudes were not given.

In our previous work on forced oscillation in RFS [10], [11], we have given very specific conditions for the design of external sinusoidal dither signals that can induce oscillations of the same frequency as this dither signal. The analysis

given was exact and does not rely on any approximation theory. The results were also necessary and sufficient. In this paper, we extend the results in [10], [11] to design sinusoidal dither signals that will result in stable oscillations of lower amplitudes than the un-dithered RFS. A bound on the dither period, T_f^* , is first determined based on the response of the linear system. For any sinusoidal dither with period $T < T_f^*$, the oscillation amplitudes in the RFS can be guaranteed to decrease monotonically with decreasing T_f . The amplitude of the dither signal can be designed based on the analysis in [10], [11]. This result is much stronger than other previous results because bounds obtained are tight and requires no approximation. It exploits the specific structure of the relay and the linear system, allowing exact responses to be written and analyzed.

The paper is organized as follows. The problem formulation is presented in Section II. Section III presents the numerical approach to identify the bound on the dither period. Complete solutions for first and second order plants will be presented in Section IV. Applications are given in Section V. Section VI presents the conclusions.

II. PROBLEM FORMULATION

Consider the RFS with a sinusoidal dither signal, $f(t)$, as shown in Fig. 1. The linear system, $G(s)$, is assumed to have a state space description and together with the relay element, the closed loop system RFS is given by

$$\dot{z}(t) = Az(t) + Bu(t - L) \quad (1)$$

$$c(t) = Cz(t)$$

$$y(t) = c(t) + f(t) = c(t) + R \sin(\omega_f t)$$

$$u(t) = \begin{cases} h & y(t) < 0 \\ -h & y(t) \geq 0 \end{cases} \quad (2)$$

where $h > 0$, $u, c \in R$ are the input and output, respectively, $z \in R^{m \times 1}$ is the state vector, $L > 0$ is the time delay between u and c , $A \in R^{m \times m}$ is Hurwitz and assumed to be non-singular, $B \in R^{m \times 1}$ and $C \in R^{1 \times m}$. In the frequency domain, $G(s) = Y(s)/U(s) = e^{-sL}C(sI - A)^{-1}B$ and $\lim_{s \rightarrow \infty} G(s) = 0$.

The problem we address is the design of $f(t)$ to achieve a reduction in the amplitude of oscillations in the RFS. The approach is based on the concept of forced oscillations (FO) [12]. Our analysis starts with the identification of the bound, T_f^* , below which the oscillation amplitude decreases monotonically as T_f decreases. Due to space constraints, the

minimum amplitude of the dither signal required to establish FO will not be shown here. However, the reader is referred to [11] for details on how to determine the minimum dither amplitude.

III. IDENTIFICATION OF T_f^*

When a RFS undergoes steady state oscillations of frequency $\omega = 2\pi/T_f$, the inputs to the linear element, $G(s)$, is a square wave with period, T_f . The response of $G(s)$ is also periodic with maximum amplitudes which are dependent on the frequency of the input square wave. The relationship between the maximum amplitudes and the frequency of the input signal is nonlinear. It is conceivable that for $G(s)$ with multiple lightly damped modes, one can expect that the function of maximum amplitudes with respect to frequency will exhibit several resonance peaks as shown in Figure 2, simulated for $G(s) = 1000/(s^5 + 6s^4 + 58s^3 + 211s^2 + 629s + 471)$. In this example, $T_f^* = 1.04$ is identified to be the first peak in Figure 2 as for $T_f < T_f^*$ the amplitude of the output of $G(s)$ decreases steadily.

In this section, a simple approach will be proposed to find T_f^* . Consider the steady state plant output, $c(t, T_f)$ for an input square wave with period T_f where

$$\begin{aligned} c(t, T_f) &= Ce^{A(t)}z(0) + \int_0^t e^{A(\tau)}u(t-L-\tau)d\tau \quad (3) \\ z(0) &= -(I + e^{A\frac{T_f}{2}})^{-1}(2e^{A(\frac{T_f}{2} - (L - n\frac{T_f}{2}))} \\ &\quad - e^{A(\frac{T_f}{2})} - I)(-1)^n A^{-1}Bh. \quad (4) \end{aligned}$$

Since this is a steady state analysis, time $t = 0$ corresponds to the positive switching edge of the relay. Suppose the maximum amplitude of $c(t, T_f)$ occurs at $t = t_0$. Then t_0 is determined by the following optimization problem :

$$t_0 = \arg \max_{t \in R} c(t, T_f). \quad (5)$$

In state space representation, the derivative of $c(t, T_f)$ is

$$\dot{c}(t, T_f) = C(Az(t) + Bu(t-L)) \quad (6)$$

and the peak amplitude occurring at $t = t_0$ can be written as :

$$c(t_0, T_f) = Ce^{At_0}z(0) + C(e^{At_0} - I)A^{-1}Bh. \quad (7)$$

To further determine the peak amplitude with respect to T_f , differentiate $c(t_0, T_f)$ with respect to T_f as follows :

$$\frac{dc(t_0, T_f)}{dT_f} = Ce^{At_0}Az(0)\frac{dt_0}{dT_f} + Ce^{At_0}\frac{dz(0)}{dT_f} + Ce^{At_0}Bh\frac{dt_0}{dT_f} \quad (8)$$

Equating (8) to zero, the turning points of $c(t_0, T_f)$ with respect to T_f can be obtained either analytically or numerically. By plotting $c(t_0, T_f)$ against T_f , the set $(0, T_f^*)$ where the amplitude of oscillation decreases monotonically with T_f can be identified. This is shown in Figure 3 for a plant with transfer function $G(s) = \frac{1}{s^2 + 2s + 20.0096}$ where $T_f^* = 0.7207$.

Once T_f^* has been identified, the remaining task is to determine the minimum amplitude of the dither signal in order for forced oscillations of the same frequency as the

dither signal to take place in the RFS. This can be done using the results in [11]. Due to space constraints, this will not be shown here. This approach guarantees that the oscillations in the RFS can be reduced if the dither signal is appropriately chosen.

In the next section, an analysis of first and second order plants will be presented to characterize the nature of T_f^* for these classes of plants.

IV. SPECIAL CASES

A. First Order Systems with Delay

In first order systems with delay, at steady state, $c(t, T_f)$ should be written in two parts due to the discontinuity resulting from the delay. With reference to (3), for $0 < \tau < L$, $u(t-L-\tau) = -h$ while for $L < \tau < \frac{T_f}{2}$, $u(t-L-\tau) = h$. By normalizing L w.r.t $T_f/2$,

$$\begin{aligned} c_1(t, T_f) &= Ce^{At}z(0) + C(e^{At} - I)A^{-1}Bh(-1)^{n+1}, \\ t &\in [0, L - n\frac{T_f}{2}] \quad (9) \end{aligned}$$

$$\begin{aligned} c_2(t, T_f) &= Ce^{At}z(0) + C(2e^{A(t-L+n\frac{T_f}{2})} - e^{At} - I) \\ &\quad A^{-1}Bh(-1)^n, t \in [L - n\frac{T_f}{2}, \frac{T_f}{2}] \quad (10) \end{aligned}$$

where $z(0)$ is given in (4) and $n = \text{floor}(\frac{2L}{T_f})$. It is assumed that the initial condition $z(0)$ corresponds to the positive switching edge of the relay at steady state. It follows that

$$\begin{aligned} \dot{c}_1(t, T_f) &= Ce^{At}Az(0) + Ce^{At}Bh(-1)^{n+1}, \\ t &\in (0, L - n\frac{T_f}{2}] \quad (11) \end{aligned}$$

$$\begin{aligned} \dot{c}_2(t, T_f) &= Ce^{At}Az(0) + C(2e^{A(t-L+n\frac{T_f}{2})} - e^{At}) \\ &\quad Bh(-1)^n, t \in [L - n\frac{T_f}{2}, \frac{T_f}{2}] \quad (12) \end{aligned}$$

Note that $z(0)$ is positive (negative) when n is odd (even) and $|Ce^{At}Az(0)| < |Ce^{At}Bh|$. Accordingly, $\dot{c}_1(t, T_f)$ is positive (negative) when n is odd (even) while $\dot{c}_2(t, T_f)$ is negative (positive) for the same n . This implies that $c(t, T_f)$ is either increasing or decreasing monotonically in each time segment and the maximum amplitude occurs at $t = L - nT_f/2$. This maximum is given by :

$$|Cz(L - n\frac{T_f}{2}, T_f)| = |C(\frac{I - e^{A\frac{T_f}{2}}}{I + e^{A\frac{T_f}{2}}})A^{-1}Bh|. \quad (13)$$

From (13), it can be seen that the amplitude $|Cz(L - n\frac{T_f}{2}, T_f)|$ decreases as $\frac{T_f}{2}$ decreases for the stable first order delayed plant where $A < 0$. This will be shown in the following example.

Example 1: Consider $G(s) = \frac{e^{-s}}{s+1}$. The undithered and dithered RFS of period $T_f = 0.8$ and 0.3 are plotted in Figure 4. It can be seen that the amplitude of the dithered system is smaller than that of the undithered case. The minimum amplitude of the dither signal required to produce the desired oscillations are $R = 0.54, 0.38$ for $T_f/2 = 0.8, 0.3$ respectively. Figure 5 plots the amplitude of the oscillation against the period of oscillation for a range of forcing periods. From the figure, it can be seen that the smaller the period of the dither signal, the smaller is the amplitude of oscillations in the RFS.

Remark 1: It is not surprising that the amplitude of oscillation increases with increasing period of the dither signal because first order plants have monotonic responses. Its first order derivative is also directly affected by the switch in the relay. Thus for each half period of the square wave input into the plant, its output increases if the half period is larger. The relationship is also monotonic.

B. Second order plants with distinct real roots

For a second order plant with distinct real roots, its state space representation in controllable canonical form is $A = [0 \ 1; -\lambda_1\lambda_2 \ (\lambda_1 + \lambda_2)]$, $B = [0 \ 1]^T$ and $C = [c_1 \ c_2]$ where $\lambda_1 < \lambda_2 < 0$ are the roots of the plant.

Following the steps in Section III, a closed form solution for t_0 is

$$t_0 = \frac{1}{\lambda_1 - \lambda_2} \Gamma \quad (14)$$

$$\Gamma = \ln\left(\frac{\lambda_1\lambda_2(c_1 + c_2\lambda_2)z_1(0) - (c_1\lambda_2 + c_2\lambda_2^2)z_2(0) - (c_1 + c_2\lambda_2)}{\lambda_1\lambda_2(c_1 + c_2\lambda_1)z_1(0) - (c_1\lambda_1 + c_2\lambda_1^2)z_2(0) - (c_1 + c_2\lambda_2)}\right).$$

For plants with pole excess of two, $c = [1 \ 0]$ and t_0 is

$$t_0 = \frac{1}{\lambda_1 - \lambda_2} \ln\left(\frac{c_1\lambda_1\lambda_2 z_1(0) - c_1\lambda_2 z_2(0) - c_1}{c_1\lambda_1\lambda_2 z_1(0) - c_1\lambda_1 z_2(0) - c_1}\right). \quad (15)$$

Substituting (15) into (8),

$$\frac{dc(t_0, T_f)}{dT_f} = e^{\lambda_1 t_0} \left(\lambda_2 \frac{dz_1(0)}{dT_f} \right) + e^{\lambda_2 t_0} \left(\frac{dz_2(0)}{dT_f} - \lambda_1 \frac{dz_1(0)}{dT_f} \right) \quad (16)$$

where $z_1(0) = \frac{-\lambda_2 \tanh(0.25\lambda_1 T_f) + \lambda_1 \tanh(0.25\lambda_2 T_f)}{\lambda_1^2 \lambda_2 - \lambda_1 \lambda_2^2}$ and $z_2(0) = \frac{-\tanh(0.25\lambda_1 T_f) + \tanh(0.25\lambda_2 T_f)}{\lambda_1 - \lambda_2}$ are the states of $z(0)$ and $t_0 = \frac{1}{\lambda_1 - \lambda_2} \ln\left(\frac{\tanh(0.25\lambda_2 T_f) - 1}{\tanh(0.25\lambda_1 T_f) - 1}\right)$.

In (16),

$$\lambda_2 \frac{dz_1(0)}{dT_f} = 0.5 \operatorname{sech}(0.25\lambda_1 T_f) > 0$$

and

$$\frac{dz_2(0)}{dT_f} - \lambda_1 \frac{dz_1(0)}{dT_f} = -0.5 \operatorname{sech}(0.25\lambda_2 T_f) < 0.$$

As $\lambda_1 < \lambda_2 < 0$, t_0 is positive and it is not difficult to see that (16) is negative, which implies that the output $c(t_0, T_f)$ is monotonically decreasing wrt T_f . The amplitude $|c(t_0, T_f)|$ increases with T_f . At large values of T_f , the plant's output signal, $c(t, T_f)$ saturates at a steady state value, much like the first order case. Thus, $T_f^* = \infty$.

Note that the Tsyarkin Locus, which plots values of $c(t, T_f/2)$ vs $\dot{c}(t, T_f/2)/\omega_f$ for different frequencies at the switching instants $t = T_f/2$, can also be used to identify T_f^* . Example 2 illustrates this.

Example 2: Consider $G(s) = \frac{1}{s^2 + 5s + 6}$, with poles at $s = -2$ and $s = -3$. The Tsyarkin Locus is shown in Figure 6(a). The magnitude of $c(T_f/2, T_f)$ increases as $T_f/2$ increases and saturates at $c(T_f/2, T_f) = -0.1667$ when $T_f^* = \infty$. The amplitude of the oscillation is plotted against $T_f/2$ in Figure 6(b). From the figure, it can be seen that the larger the period of oscillation, the larger the amplitude.

C. Second order plant with complex roots

For a second order plant with complex roots, denoted by $a \pm ib$, its state space representation can be written as $A = [0 \ 1; -(a^2 + b^2) \ 2a]$, $B = [0 \ 1]^T$, $C = [c_1 \ c_2]$. For plants with pole excess of two, $c = [1 \ 0]$ and the turning point t_0 of the output is given by

$$t_0 = \frac{1}{b} \tan^{-1}\left(\frac{bz_2(0)}{(a^2 + b^2)z_1(0) - az_2(0) - 1}\right) \quad (17)$$

For $t = t_0$, the output amplitude for varying T_f is given by (7). The bound T_f^* where the amplitude of oscillation $c(t_0, T_f)$ decreases monotonically with T_f for the set $(0, T_f^*)$ is determined by equating (8) to zero, which gives $\frac{T_f}{2} = \frac{m\pi}{b}$ where $m \in \mathbb{N}^+$. Thus, for a second order system with complex roots, the amplitude of the limit cycle decreases monotonically with decreasing period for $T_f \in (0, T_f^*)$ where $T_f^* = \frac{2m\pi}{b}$.

At $\frac{T_f}{2} = \frac{m\pi}{b}$, $z_2(0) = 8b(a^2 + b^2)e^{a\frac{T_f}{2}} \sin b\frac{T_f}{2} = 0$ and $t_0 = 0$ or $t_0 = T_f/2$ in (17). Hence, the value of T_f^* can also be identified from the Tsyarkin Locus, which plots values of $c(t, T_f)$ and $\dot{c}(t, T_f)/\omega_f$ at $t = T_f/2$ for varying T_f . This is demonstrated in the following example.

Example 3: Consider a second order plant with transfer function, $G(s) = \frac{1}{s^2 + 2s + 20.0096}$, with complex roots at $s = -1 \pm 4.36i$. The Tsyarkin Locus in Figure 7(a) shows that the outer spiral with $c(T_f/2, T_f)$ increases in magnitude from zero to about 0.15 before spiralling in with lower magnitudes. Hence the maximum T_f corresponding to maximum magnitude can be determined by the point which crosses the y-axis or the point corresponding to $\dot{c}(T_f/2, T_f) = 0$. This gives $T_f^*/2 = 0.7207$. The amplitude of the oscillation is plotted against the period of oscillation in Figure 7(b) which verifies the results obtained from the Tsyarkin Locus. From the figure, it can be seen that for $T_f^*/2 = 0.7207$, the maximum amplitude is about 0.15.

D. Second order plant with repeated roots

For a second order system with repeated roots at λ_1 , its state space representation is $A = [0 \ 1; -\lambda_1^2 \ 2\lambda_1]$, $b = [0 \ 1]^T$, $c = [c_1 \ c_2]$ where $\lambda_1 < 0$.

For plants with pole excess of 2, t_0 is given by

$$t_0 = \frac{-z_2(0)c_1}{z_2(0)\lambda_1 c_1 - \lambda_1^2 z_1(0)c_1 + c_1} \quad (18)$$

and the change in the output amplitude $\frac{dc(t_0, T_f)}{dT_f}$ given by

$$C e^{A t_0} \frac{dz(0)}{dT_f} = e^{\lambda_1 t_0} \left(\frac{dz_1(0)}{dT_f} - \lambda_1 t_0 \frac{dz_1(0)}{dT_f} + t_0 \frac{dz_2(0)}{\partial T_f} \right). \quad (19)$$

The states of $z(0)$ are given by $z_1(0) = \frac{-0.5\lambda_1 T_f + \sinh(\lambda_1 T_f)}{\lambda_1^2(1 + \cosh(0.5\lambda_1 T_f))}$ and $z_2(0) = \frac{0.5T_f}{1 + \cosh(0.5\lambda_1 T_f)}$. From (18), $t_0 = \frac{0.5T_f}{-\sinh(0.5\lambda_1 T_f) + 1 + \cosh(0.5\lambda_1 T_f)}$, which is positive. The factor in (19),

$$\begin{aligned} & \frac{dz_1(0)}{dT_f} (1 - \lambda_1 t_0) + t_0 \frac{dz_2(0)}{dT_f} \\ &= \frac{0.5T_f \sinh(0.5\lambda_1 T_f)}{(1 + \cosh(0.5\lambda_1 T_f))^2} - t_0 \left(\frac{1}{\cosh(0.5\lambda_1 T_f)} \right) \end{aligned} \quad (20)$$

is negative, which implies that the output $c(t_0, T_f)$ is monotonically decreasing and the amplitude $|c(t_0, T_f)|$ increases with T_f . Thus, $T_f^* = \infty$. The value of $T_f^*/2$ can also be identified from the Tsytkin Locus. This result is the same as that for two second order plants with real and distinct roots.

E. Higher order non-delayed plants

As shown in the first and second order cases, the Tsytkin Locus is a good way to determine T_f^* if t_0 is known. For higher order systems, t_0 may not coincide with 0 or $T_f/2$, unlike the first and second order systems. The delayed version of the Tsytkin Locus, which is the plot of $c(t_0, T_f)$ against $\dot{c}(t_0, T_f)/\omega_f$ can actually be used to determine t_0 and the set $(0, T_f^*)$ where the amplitude decreases monotonously with period. If we plot the delayed Tsytkin Locus for a series of t_0 and identify t_0 where $c(t_0, T_f)$ reaches its maximum amplitude, T_f^* will be the point corresponding to $\dot{c}(t_0, T_f) = 0$. An example is shown to illustrate this point.

Example 4: Consider a fourth order plant with transfer function, $G(s) = \frac{1}{s^4 + 6s^3 + 23s^2 + 20s + 26}$, with complex roots at $s = -2.657 \pm 3.2928i$ and $s = -0.343 \pm 1.1553i$. A series of the delayed Tsytkin Locus, $c(t_0, T_f)$ against $\dot{c}(t_0, T_f)/\omega_f$ is plotted for $t_0 = 0.05, 0.1, 0.15, 0.2049, 0.25, 0.3$, as shown in Figure 8(a). An amplification of the plot in Figure 8(b) shows that the maximum magnitude of $c(t_0, T_f)$ is 0.0893 and it occurs at $t_0 = 0.2049$. The "boxed" frequency point at which the Tsytkin Locus, $c(0.2049, T_f)$ vs $\dot{c}(0.2049, T_f)$ crosses the imaginary axis or the point corresponding to $\dot{c}(0.2049, T_f) = 0$ is $T_f = 2.76$. This gives $T_f^* = 2.76$.

V. APPLICATIONS

In this section, the analysis of two motivating examples will be presented and a comparison between the performance of different dither shapes will be carried out.

Example 5: The following problem is posed by [13], converted to SI units by [14] and adapted to illustrate our problem. The block diagram is shown in Figure 9 where $F_0 = 445N$, $R_0 = 0.61m$, $J = 4.68N \cdot m/s^2$, $h = 22.24N$, $K_p = 1868N/radian$ and $K_v = 186.8N \cdot /radian$. The self oscillation and dithered response are shown in Figure 10 where $T_f/2 = 0.037$ and amplitude of 0.55. It can be verified that the oscillations are indeed reduced. Figure 11 plots $c(t, T_f)$ with sinusoidal dither and sawtooth dither where $T_f/2 = 0.037$. It can be seen that the oscillation amplitudes are the same in both cases.

Example 6: Consider the case of a DC motor whose model is given in Figure 12 (adapted from [2]). The closed loop transfer function is

$$\frac{k_t k_{pot} V_a L}{J L L_a s^3 + (\beta L + R_1 J) L_a s^2 + (\beta R_1 + k_t k_e) L_a s}$$

The system exhibited self oscillation, FO and SO with the following set of parameters. $V_a = 5V$, $R_1 = 2.510\Omega$, $L_a = 0.530mH$, $k_t = k_e = 5.700mV/rad \cdot s^{-1}$, $\beta = 0.411mN \cdot cm/rad \cdot s^{-1}$, $J = 31.400g \cdot cm^2$, $k_{pot} = 3/2\pi V/rad$, $T_f/2 = 0.005$ and amplitude 0.05. It is shown in Figure

13 that the amplitudes of the oscillations are indeed reduced with a dither frequency higher than that of self oscillation. Figure 14 plots the oscillation amplitudes for a sine dither and a sawtooth dither where the dither amplitudes are 0.07 and frequencies at 100 Hz. It can be seen that the oscillation amplitudes are the same in both cases.

VI. CONCLUSION

In this paper, the potential of using a sinusoidal dither in reducing inherent system oscillations has been illustrated. The bound on the dither period T_f^* was determined both numerically and analytically for the first and second order plants. For the higher order systems, the Tsytkin Loci was used to identify T_f^* . Reduced oscillations of the desired frequency were achieved with the corresponding dither amplitude required. The reduction in oscillation amplitude by the sinusoidal dither is seen to be significant.

REFERENCES

- [1] Luigi Iannelli, Karl Henrik Johansson, Ulf T. Jönsson, Francesco Vasca, "Dither for Smoothing Relay Feedback Systems", IEEE Transactions on Circuits and Systems Part I, vol. 50, no. 8, pp 1025-1035, August 2003
- [2] Luigi Iannelli, Karl Henrik Johansson, Ulf T. Jönsson, Francesco Vasca, "Effects of Dither Shapes in Nonsmooth Feedback Systems: Experimental Results and Theoretical Insight", Proceedings of the 42nd IEEE Conference on Decision and Control, pp 4285-4290, 2003
- [3] A. A. Pervozvanski, C. Canudas de Wit, "Asymptotic analysis of the dither effect in systems with friction", Automatica, vol. 38, no. 1, pp 105-113, January 2002
- [4] G. Zames, P.L.Falb, "Stability conditions for systems with monotone and slope restricted nonlinearities", Sian J. Control, vol. 6, no. 1, 1968
- [5] G. Zames, N.A. Shneydor, "Structural Stabilization and Quenching by Dither in Nonlinear Systems", IEEE Transactions on Automatic Control, Vol. AC-22, No. 3, June 1977
- [6] G. Zames, N.A. Shneydor, "Dither in Nonlinear Systems", IEEE Transactions on Automatic Control, vol. AC-21, no. 5, October 1976
- [7] Mossaheb S, "Application of a method of averaging to the study of dither in non-linear systems", International Journal of Control, vol. 38, no. 3, pp 557-576, 1983
- [8] Luigi Iannelli, Karl Henrik Johansson, Ulf T. Jönsson, Francesco Vasca, "Averaging of nonsmooth systems using dither", Automatica, vol. 42, pp 669-676, 2006
- [9] Brad Lehman, Richard M. Bass, "Extensions of Averaging Theory for Power Electronic Systems", IEEE Trans on Automatic Control, vol. 11, no. 4, July 1996
- [10] Loh A P, Fu Jun, Tan W W, "Controller Design for TITO Systems with Mode3 Oscillations", In Proceedings of the IEE International Conference on Control 2000, Cambridge, UK, September, 2000
- [11] Lim L H, Loh A P, Fu J, "Estimation of Minimum Conditions for Forced Oscillation in Relay Feedback Systems", ICCA, pp 1262-1267, 2005
- [12] Tsytkin Y Z, *Relay Control Systems*, Cambridge University Press, 1984.
- [13] J E Gibson, "Nonlinear Automatic Control (International Student Edition)", McGraw-Hill Book Company, 1963
- [14] James H. Taylor, "Electrical and Electronics Engineering Encyclopedia, Supplement 1", John Wiley & Sons, Inc., 2000

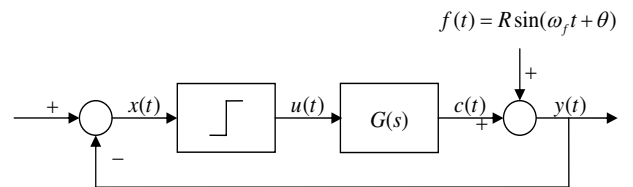


Fig. 1. Single loop with external forcing signal.

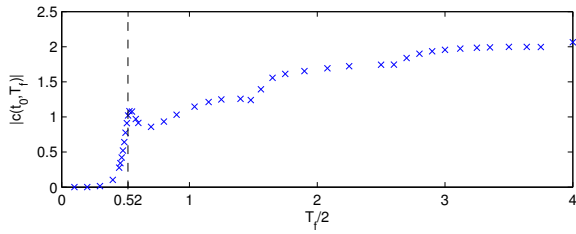


Fig. 2. Plot of the amplitude of oscillation against $T_f/2$ for $G(s) = 1000/(s^5 + 6s^4 + 58s^3 + 211s^2 + 629s + 471)$.

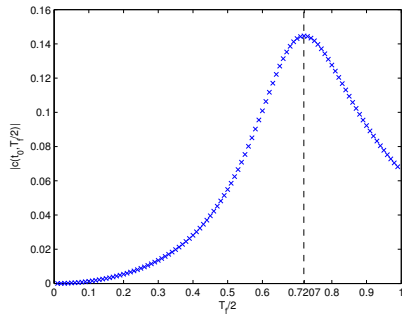


Fig. 3. Plot of the amplitude of oscillation against $T_f/2$ for $G(s) = \frac{1}{s^2 + 2s + 20.0096}$.

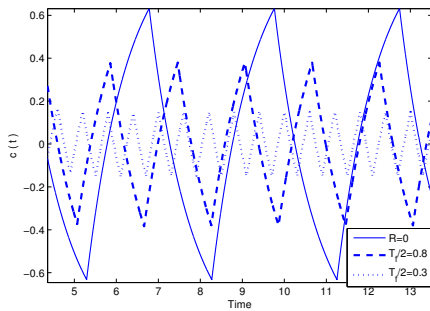


Fig. 4. Self oscillation and FO of differing $T_f/2$ in example 1.

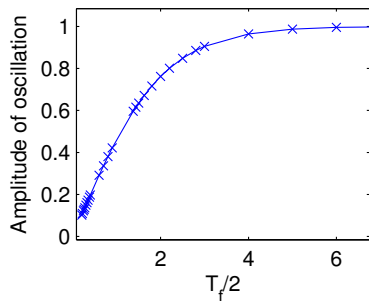


Fig. 5. Plot of the amplitude of oscillation against $T_f/2$ in example 1.

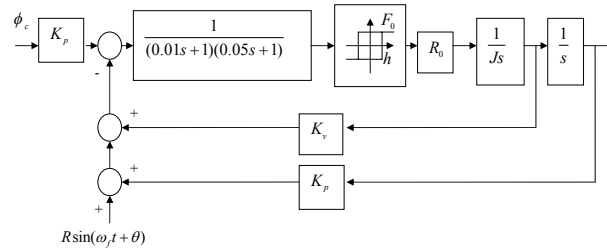


Fig. 9. Block diagram of the Missile Roll-Control problem. [14]

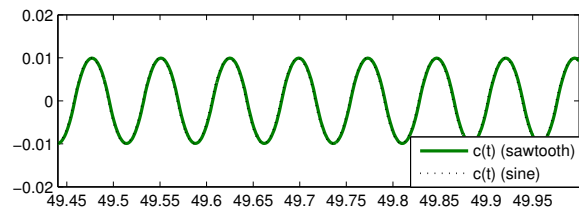


Fig. 11. Plot of $c(t)$ with sine and sawtooth dither

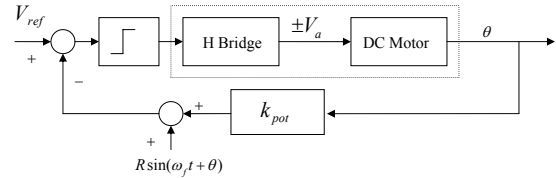


Fig. 12. Model of the DC motor in example 6.

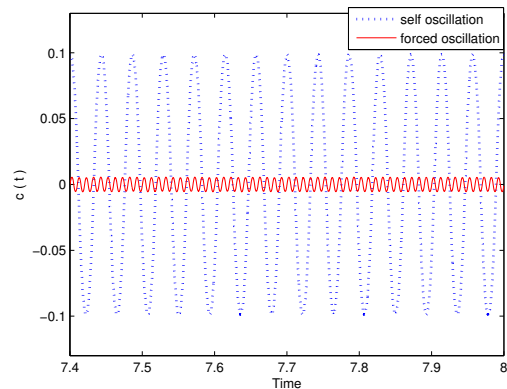


Fig. 13. Comparison of the oscillation amplitudes of the DC motor in example 6.

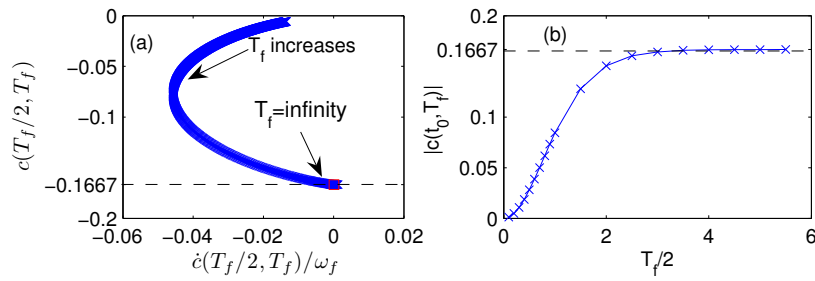


Fig. 6. (a)Plot of the Tsytkin Locus in example 2. (b)Plot of the amplitude of oscillation against $T_f/2$ in example 2.

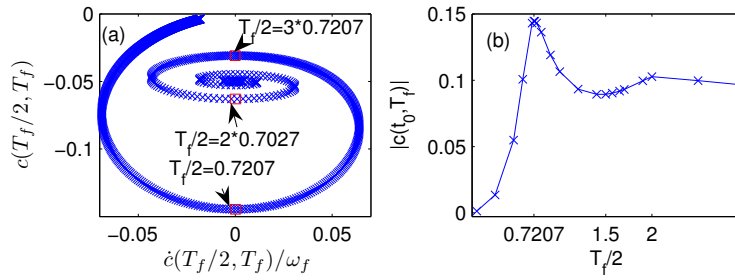


Fig. 7. (a)Plot of the Tsytkin Locus in example 3. (b)Plot of the amplitude of oscillation against $T_f/2$ in example 3.

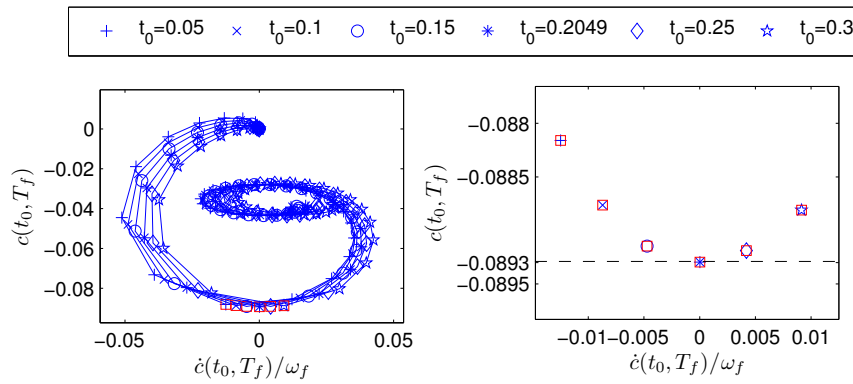


Fig. 8. (a)Plot of the delayed Tsytkin Locus in example 4. (b)Amplification of the delayed Tsytkin Locus in example 4.

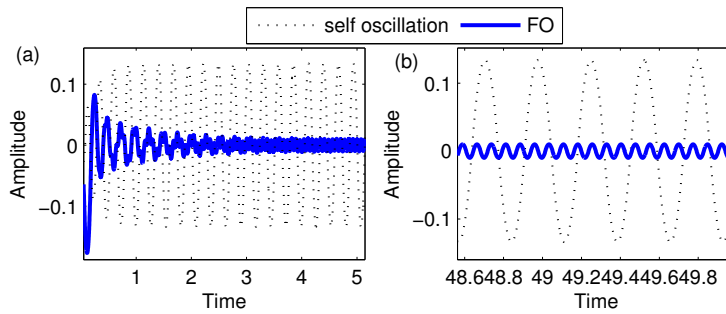


Fig. 10. (a)Comparison of the oscillation amplitudes in example 5. (b)Comparison of the steady state oscillation amplitudes in example 5.

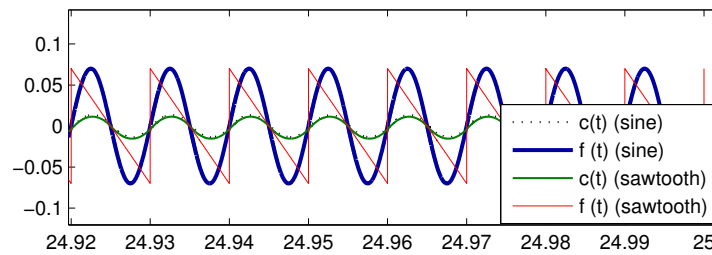


Fig. 14. Comparison of the oscillation amplitudes between the sine and sawtooth dithers in example 6.